Nuclear Instruments and Methods in Physics Research B10/11 (1985) 247–252
North-Holland, Amsterdam

TRIPLY DIFFERENTIAL PHOTOELECTRON STUDIES OF RESONANCES IN MOLECULAR PHOTOIONIZATION *

J.L. DEHMER and S.H. SOUTHWORTH

Argonne National Laboratory, Argonne, IL 60439, USA

A.C. PARR

Synchrotron Ultraviolet Radiation Facility, National Bureau of Standards, Gaithersburg, MD 20899, USA

Shape and autoionizing resonances are central to the study of molecular photoionization for various reasons, the most obvious one being that they are usually displayed prominently against nonresonant behavior in such observables as the total photoionization cross section, photoionization branching ratios, and photoelectron angular distributions. More importantly, the study of resonant features has repeatedly led to a deeper physical insight into the mechanisms of excitation, resonant trapping of the photoelectron, and decay of the excited complex that occur during the photoionization process. A major impetus has been provided in this area by the ability to freely probe resonances throughout the ionization continuum with synchrotron radiation and to perform angle-resolved photoelectron spectrometry on the ejected electrons. Selected examples will serve to illustrate the recent progress and the prospects of this stream of work.

1. Introduction

The last decade has witnessed remarkable progress in characterizing dynamical aspects of molecular photoionization (see, e.g., refs. [1] and [2] and references therein). The general challenge is to gain physical insight into the processes occurring during photoexcitation and the eventual escape of the photoelectron through the anisotropic molecular field in terms of various physical observables such as photoionization cross sections, branching ratios, and photoelectron angular distributions. Throughout this work, special attention is invariably drawn to resonant processes, in which the excited system is temporarily trapped in a quasi-bound resonant state. Such processes tend to amplify the more subtle dynamics of excited molecular states. Much of the progress in this field has mirrored earlier work in atomic photoionization dynamics where many key ideas were developed, e.g., channel interaction, quantum defect analysis, potential barrier phenomena, and experimental techniques. However, additional concepts and techniques were required to deal with the strictly molecular aspects of the problem, particularly the anisotropy of the multicenter molecular field and the interaction among rovibronic modes.

Experimentally, one of the most important factors in this field has been the ability to make angle-resolved photoelectron measurements using synchrotron radiation. Such measurements are now very often vibrationally resolved, giving access to information on the interactions between electronic and vibrational modes. On the theoretical side, the development of realistic methods of computing continuum wave functions in anisotropic molecular fields [3], and the adaptation of multichannel quantum defect theory to molecular photoionization [4,5] have complemented and stimulated the experimental progress. Here we will employ selected examples from recent work to illustrate the progress and prospects in this very active stream of research.

2. Triply differential photoelectron measurements

By triply differential photoelectron studies, we mean that photoelectron intensity measurements are made as a function of three completely independent variables – the incident wavelength, λ, the kinetic energy of the ejected electron, T, and the angle of ejection, θ, relative to the polarization direction of the light. *Variation of* λ permits exploration of photoionization properties throughout the photoionization continuum, including probing important spectral features such as autoionizing states, shape resonances, and near-threshold phenomena. Clearly, synchrotron radiation plays a key role in providing access to phenomena at all wavelengths from the lowest ionization potential all the way to deep inner shells, which can only be probed by hard X-rays. *Variation of* T permits the selection of particular

* Work supported by the Office of Naval Research and the US Department of Energy.

electronic–vibrational–(rotational) states formed in the photoionization process. Hence, by monitoring the whole manifold of final states (different T's), one can determine the effect of alternative photoionization mechanisms (selected by choosing λ, as discussed above) on relative probabilities of forming the various final states. *Variation of* θ permits the characterization of the angular distribution of photoelectrons for each final state and λ. In the photoionization of randomly oriented atoms and molecules the angular dependence of photoelectron intensity has the simple form

$$\frac{d\sigma}{d\theta} = \frac{\sigma_{tot}}{4\pi}[1 + \beta P_2(\cos\theta)],$$

where σ_{tot} is the integrated cross section and β is called the asymmetry parameter. Therefore, the angular distribution as a function of (T, λ) can be characterized by β, which in turn can be measured by recording peak strengths at as little as two angles. While it is true that many applications of photoionization data hinge primarily on partial cross sections (or branching ratios), angular distributions play an indispensable role in testing theoretical models and in the fundamental understanding of the photoionization process. Hence, both branching ratios and β's are critical to a sound scientific study of photoionization processes.

A new, high-resolution, double analyzer system [6] recently installed at the National Bureau of Standard's SURF-II synchrotron radiation facility is shown schematically in fig. 1. A special feature of this new instrument is its high resolving power (~ 10 meV under good signal conditions), which will permit routine separation of vibrational structure in polyatomic molecules. Analogous systems, with differently optimized characteristics, are operating in more than a half dozen synchrotron radiation facilities around the world.

3. Shape resonances – background

Shape resonances are quasibound states in which a particle is temporarily trapped by a potential barrier, through which it may eventually tunnel and escape. In molecular fields, such states can result from so-called "centrifugal barriers," which block the motion of otherwise free electrons in certain directions, trapping them in a region of space with molecular dimensions. Over the past ten years, this basic resonance mechanism has

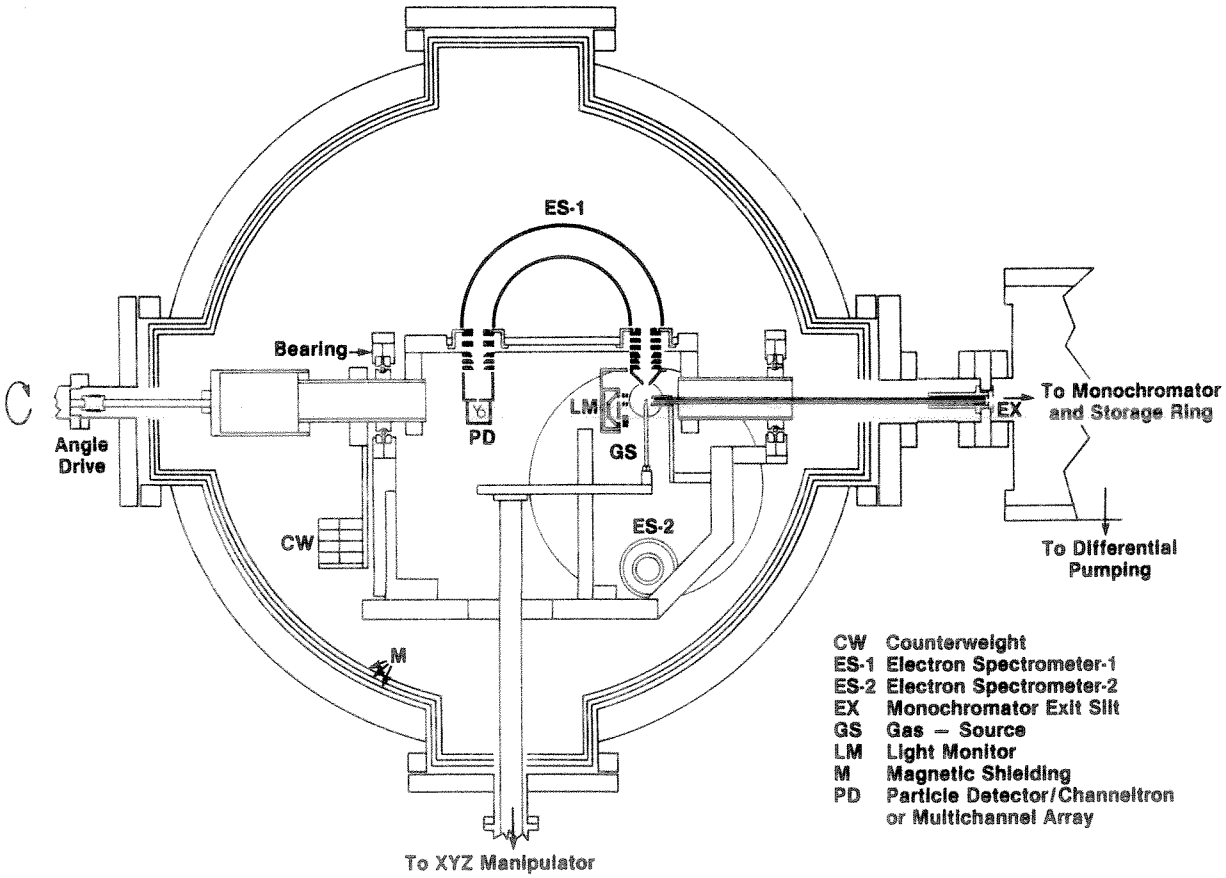

Fig. 1. Schematic diagram of high-resolution, double electron spectrometer system (from ref. [6]).

been found to play a prominent role in a variety of processes in molecular physics. As discussed more fully elsewhere [1], the expanding interest in shape resonant phenomena has arisen from a few key factors: first, shape resonance effects are being identified in the spectra of a growing diverse collection of molecules and now appear to be active somewhere in the observable properties of most small (nonhydride) molecules. Second, being quasibound inside a potential barrier on the perimeter of the molecule, such resonances are localized, have enhanced electron density in the molecular core, and are uncoupled from the external environment of the molecule. This localization often produces intense, easily studied spectral features, while suppressing non-resonant and/or Rydberg structure and, as discussed more fully below, has a marked influence on vibrational motion. Third, resonant trapping by a centrifugal barrier often imparts a well-defined orbital momentum character to the escaping electron. This can be directly observed and shows that the centrifugal trapping mechanism has physical meaning and is not merely a theoretical construct. Fourth, the predominantly one-electron nature of the phenomena lends itself to theoretical treatment by realistic, independent-electron methods [1–3], with the concomitant flexibility in terms of complexity of molecular systems, energy ranges, and alternative physical processes. This has been a major factor in the rapid exploration in this area.

The extensive progress in understanding shape resonance behavior at the independent-electron, fixed nuclei level of approximation has been the subject of recent reviews (refs. [1,2] and references therein), and will not be detailed further here. Rather, we turn to a hierarchy of departures from this level of approximation. First, we consider non-Franck–Condon vibrational effects induced by shape resonances. Second, we discuss how channel interaction alters the independent electron picture of shape resonances.

4. Shape-resonance-induced non-Franck–Condon effects

Once the independent-electron, fixed-nuclei model of molecular shape resonance phenomena was qualitatively understood, it was of great interest to explore other manifestations of this widespread mechanism. An immediate question is to what extent does this electronic trapping mechanism effect vibrational behavior, e.g., does it cause non-Franck–Condon effects? To ask what effect shape resonances have on vibration is equivalent to asking how shape resonances vary with internuclear separation. This was studied adiabatically by computing the σ_u shape resonance profile in the process

$$N_2 X^1\Sigma_g^+ + h\nu \rightarrow N_2^+ X^2\Sigma_g^+ + \epsilon\sigma_u$$

corresponding to ionization of the outermost $3\sigma_g$ orbital of N_2 [7]. What was found is a strong dependence of the resonance width and position as a function of R. This sensitivity results from the localization of the shape resonance by a centrifugal barrier which is comprised of delicately balanced attractive and repulsive forces, as discussed elsewhere [1,7]. The net result is that the partial photoionization cross sections and resulting branching ratios were predicted to deviate strongly from Franck–Condon behavior over a broad spectral range, several times the resonance halfwidth. Non-Franck–Condon behavior of $\beta(v)$ was also predicted.

These theoretical predictions were soon tested experimentally. In fig. 2 the branching ratio for production of the $v = 0$ and 1 vibrational levels of $N_2^+ X^2\Sigma_g^+$ is shown. The dash–dot line is the original prediction [7]. The solid dots are the measurements [8] in the vicinity of the shape resonance at $h\nu \sim 30$ eV. The conclusion drawn from this comparison is that the observed variation of the vibrational branching ratio relative to the Franck–Condon factor qualitatively confirms the prediction; however, subsequent calculations [10] with fewer approximations have achieved far better agreement, though still based on the same mechanism for breakdown of the Franck–Condon separation. The dashed and solid curves in fig. 2 are results based on a Schwinger variational treatment [10] of the photoelectron wavefunction. The two curves represent length and velocity representations of the transition matrix element, both of which are in excellent agreement with the data. This is an outstanding example of interaction between experiment and theory, proceeding as it did from a novel prediction, through experimental testing, and final quantitative theoretical agreement in a short time.

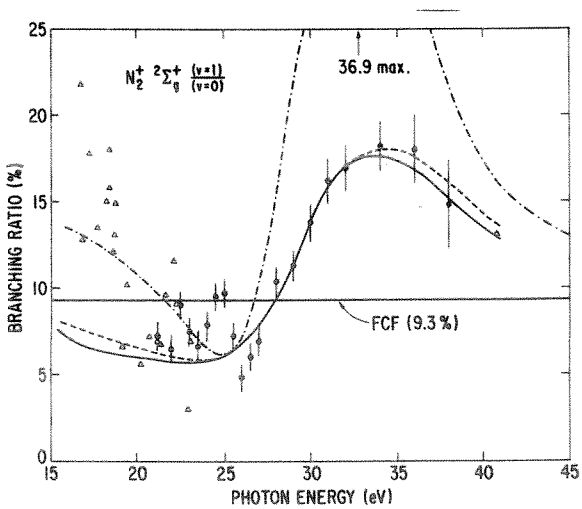

Fig. 2. Branching ratios for production of the $v = 0$, 1 levels of $N_2^+ X^2\Sigma_g^+$ by photoionization of N_2: ●, data from ref. [8]; Δ, data from ref. [9]; –·–·–, multiple scattering model prediction from ref. [7]; ———, - - -, frozen-core Hartree–Fock dipole length and velocity approximation calculations from ref. [10].

5. Continuum-continuum coupling

A very recent addition to the body of information on shape resonances involves departures from the behavior expected on the basis of independent electron reasoning. An example will serve to illustrate the point. In SF_6, the sulfur $L_{2,3}$ spectra [11,12] show extremely intense t_{2g} and e_g shape resonances lying ~ 3 eV and ~ 15 eV above the L-shell ionization limit. Since these are quasibound states in the respective continua (i.e., a final state effect), it is reasonable to expect that these same states would be prominent in valence shell photoionization channels in which they are dipole-allowed. A shift of 1 to 4 eV to higher kinetic energy is to be expected due to differences in screening between core and valence shell vacancies. In fact, the t_{2g} is observed [13,14] in the $1t_{2u}$, $5t_{1u}$, and $4t_{1u}$ (dipole-allowed) photoionization channels, but it also appears with sizable strength in the $1t_{1g}$ and $3e_g$ channels, where it is dipole forbidden in the independent-electron approximation. Figs. 3 and 4 show the results [14] of an independent-electron calculation and a recent triply-differential photoelectron measurement. In the lower frame of fig. 3, the solid curve (the dashed curve in figs. 3 and 4 corresponds to a possible alternative assignment, which is discussed in ref. [14], but which can be eliminated on the basis of X-ray data) shows the partial cross section for the second peak in the photoelectron spectrum of

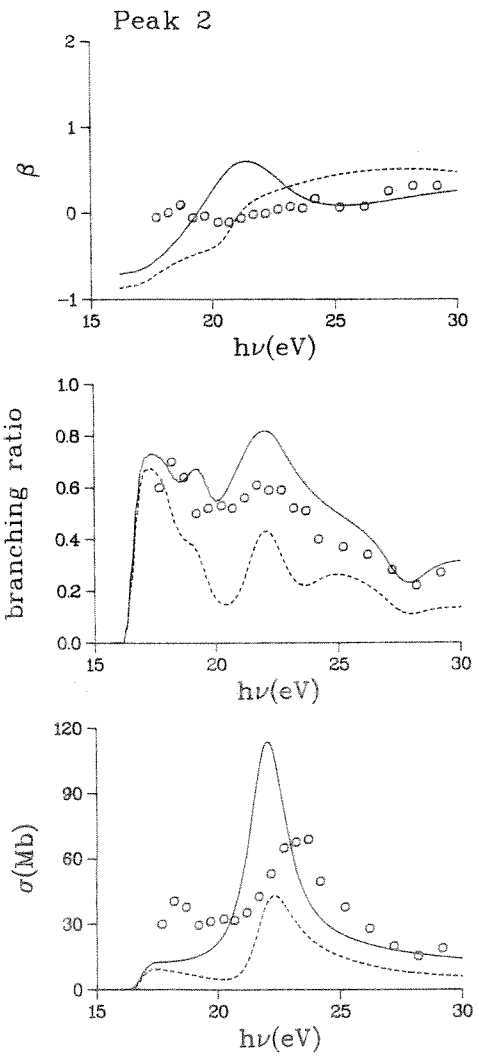

Fig. 3. Photoelectron asymmetry parameter, branching ratio, and partial cross section for photoelectron peak 2 (IP = 17.0 eV) of SF_6. Open circles are data from ref. [14]. Curves are theoretical calculations discussed in the text.

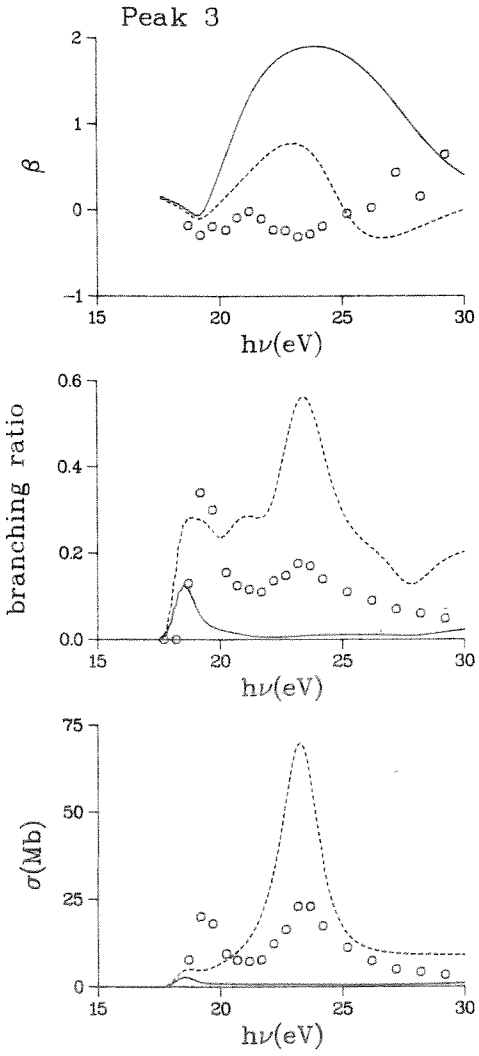

Fig. 4. Photoelectron asymmetry parameter, branching ratio, and partial cross section for photoelectron peak 3 (IP = 18.6 eV) of SF_6. Open circles are data from ref. [14]. Curves are theoretical calculations discussed in the text.

SF_6. The large resonance is attributable to transitions from the degenerate $5t_{1u}$ and $1t_{2u}$ orbitals to the ϵt_{2g} shape resonance, and qualitative agreement between theory and experiment is observed. In fig. 4 (lower frame), however, the solid curve shows the independent electron result for the $3e_g$ partial cross section. In this channel, the ϵt_{2g} shape resonance is not dipole allowed in the independent-electron approximation; however, the data show a resonance at the same *photon energy* as the large peak in fig. 3. Note that the intensity of the t_{2g} peak in fig. 4 is approximately equal to the difference between the t_{2g} peaks in the theoretical and experimental curves in fig. 3. This observation, attributed [14] to continuum–continuum coupling, complicates the use of shape resonances to assign the symmetries of photoelectron peaks, at least in valence shell spectra. Even more problematic, the e_g shape resonance is not clearly seen in valence shell partial cross sections [13] at all! The cause for this is still unknown.

Another dramatic example of continuum–continuum coupling has just been described by Stephens and Dill [15], this time in N_2 photoionization. In this case the $2\sigma_u$ photoionization channel is shown to exhibit shape resonance effects which are attributable to coupling to the resonance in the $\epsilon\sigma_u$ continuum. This would be forbidden for $2\sigma_u$ photoionization in the independent electron approximation, but can arise from short range electron correlation in the excited molecular complex. This recent work tentatively explains the puzzling behavior of the β for this channel [16], but more extensive theoretical and experimental studies are needed to confirm this effect.

6. Molecular autoionization

Autoionization is an intrinsically multichannel process in which a resonantly excited discrete state from one channel couples to the underlying electronic continua of one or more other channels to effect ionization. It has been known since Fano's original work [17], almost fifty years ago, that this process produces characteristic asymmetric Fano–Beutler profiles in the photoionization cross section. Since then, there have been extensive studies of autoionization structure in the photoionization spectra of atoms and molecules. In addition, the manifestations of autoionization in such dynamical parameters as photoionization branching ratios and photoelectron angular distributions have been recognized (see, e.g., refs. [18] and [19]) and have recently developed into a major focal point for current studies of molecular photoionization dynamics. With recent improvements in instrumentation, this subfield is poised for a major advance when the dynamics of molecular autoionization can be fully probed using synchrotron radiation and triply differential photoelectron spectrometry.

A more physical description of the autoionization process is helpful in discussing the alternative decay mechanisms possible in molecules: in most cases, autoionizing states consist of an excited Rydberg electron bound to an excited ion (also called the core) primarily by Coulomb attraction. A necessary condition for the decay of this state by ionization is that the excitation energy of the ion is greater than the binding energy of the Rydberg electron. Then, barring alternative decay paths, autoionization will take place by means of a close collision, between the Rydberg electron and the ion, in which excitation energy of the ion is transferred to the excited electron to overcome its binding energy and permit its escape from the ionic field. Notice that, although a Rydberg electron spends only a very small fraction of time within the molecular ion, such close encounters are essential for autoionization since, only when the Rydberg electron is nearby, can it participate fully in the dynamics of the core and exchange energy efficiently with it.

A molecular ion core can store the energy needed to ionize a Rydberg electron in any of its three modes – electronic, vibrational, or rotational. The most direct means of storing electronic energy is to produce a hole in a molecular orbital (MO) other than the outermost occupied MO, e.g., by promoting one of these inner electrons into the Rydberg orbital to prepare the autoionizing state in the first place. In addition, various degrees of vibrational and rotational excitation can accompany photoexcitation of Rydberg states converging to any state of the ion. It is the existence and interplay among the alternative energy modes which lead to the unique properties of molecular autoionization.

Significant advances, both in theory and experiment, have been made over the past few years, including MQDT calculations on small diatomics (see, e.g., refs. [18,19]) and prototype measurements on N_2 (see, e.g., ref. [20]). The only comparison between experiment and theory involves the Hopfield series in N_2 [19]. This comparison exhibited qualitative agreement, but underscored the need for improved data and further progress in theory. A very pressing challenge is the experimental testing of theoretical predictions by Raoult and Jungen [18] of vibrational branching ratios and $\beta(v)$ for vibrational autoionization in the most fundamental molecular system, H_2. This is a widely recognized problem, requiring higher photon resolution, $\Delta\lambda \lesssim 0.1$ Å, than is commonly available with sufficient intensity at synchrotron radiation sources. We will soon attempt this study with a new 4800 l/mm grating, which should provide sufficient resolution to test the theoretical predictions. Obviously, this is just the tip of the iceberg in this research area, and much progress is anticipated in the near future.

References

[1] J.L. Dehmer, D. Dill and A.C. Parr, in: Photophysics and Photochemistry in the Vacuum Ultraviolet, eds., S. McGlynn, G. Findley and R. Huebner (Reidel, Dordrecht, 1985) p. 341.

[2] V. McKoy, T.A. Carlson and R.R. Lucchese, J. Phys. Chem. 88 (1984) 3188.

[3] T. Rescigno, V. McKoy and B. Schneider, eds., Electron–Molecule and Photon–Molecule Collisions (Plenum, New York, 1979).

[4] U. Fano, J. Opt. Soc. Am. 65 (1975) 979.

[5] D. Dill and Ch. Jungen, J. Phys. Chem. 84 (1980) 2116.

[6] A.C. Parr, S.H. Southworth, J.L. Dehmer and D.M.P. Holland, Nucl. Instr. and Meth. 222 (1984) 221.

[7] J.L. Dehmer, D. Dill and S. Wallace, Phys. Rev. Lett. 43 (1979) 1005.

[8] J.B. West, A.C. Parr, B.E. Cole, D.L. Ederer, R. Stockbauer and J.L. Dehmer, J. Phys. B13 (1980) L105.

[9] J.L. Gardner and J.A.R. Samson, J. Electron Specrosc. 13 (1978) 7.

[10] R.R. Lucchese and B.V. McKoy, J. Phys. B14 (1981) L629.

[11] T.M. Zimkina and V.A. Fomichev, Sov. Phys. Dokl. 11 (1966) 726.

[12] J.L. Dehmer, J. Chem. Phys. 56 (1972) 4496.

[13] H.J. Levinson, T. Gustafsson and P. Soven, Phys. Rev. A19 (1979) 1089.

[14] J.L. Dehmer, A.C. Parr, S. Wallace and D. Dill, Phys. Rev. A26 (1982) 3283.

[15] J.A. Stephens and D. Dill, to be published.

[16] G.V. Marr, J.M. Morton, R.M. Holmes and D.G. McCoy, J. Phys. B12 (1979) 43.

[17] U. Fano, Nuovo Cimento 12 (1935) 156.

[18] M. Raoult and Ch. Jungen, J. Chem. Phys. 74 (1981) 3388.

[19] M. Raoult, H. Le Rouzo, G. Raseev and H. Lefebvre-Brion, J. Phys. B16 (1983) 4601.

[20] A.C. Parr, D.L. Ederer, B.E. Cole, J.B. West, R. Stockbauer, K. Codling and J.L. Dehmer, Phys. Rev. Lett. 46 (1981) 22.